Electric Power Systems Research xxx (2016) xxx–xxx

Contents lists available at ScienceDirect

Electric Power Systems Research

journal homepage: www.elsevier.com/locate/epsr

Derivation and evaluation of generic measurement-based dynamic load models

Konstantinos S. Metallinos [a], Theofilos A. Papadopoulos [b,*], Charalambos A. Charalambous [a]

[a] Department of Electrical and Computer Engineering, Faculty of Engineering, University of Cyprus, PO Box 20537, 1687 Nicosia, Cyprus
[b] Power Systems Laboratory, Department of Electrical and Computer Engineering, Democritus University of Thrace, 67100 Xanthi, Greece

ARTICLE INFO

Article history:
Received 25 January 2016
Received in revised form 10 April 2016
Accepted 9 June 2016
Available online xxx

Keywords:
Artificial neural networks
Generic models
Load modelling
Measurement-based approach
Nonlinear least-square optimization
Statistical analysis

ABSTRACT

Online recorded responses can be used for aggregate dynamic load modelling, taking advantage of the advent of smart grids and the growing installation of phasor measurement units. Although several measurement-based dynamic load models have been proposed in the literature, still most network utilities and system operators take advantage of well-known formulations such as the polynomial and the exponential recovery models. However, these types of load models are only valid for a specific range of operating conditions, thus minimizing their applicability and efficiency. This is mainly due to the fact that the model parameter estimation procedure relies on iterative processes. To this extent, the specific scope of this paper is to present a comprehensive identification procedure for evaluating load models under different loading conditions and further to propose two generic modelling approaches that can be used to derive robust load models that are suitable for dynamic simulations over a wide range. Towards achieving the scope of this paper, Monte Carlo simulations are used to train and validate the data of the loading conditions. Finally, several simulations are performed within the DIgSILENT PowerFactory software to assess the accuracy of the proposed models.

1. Introduction

Aggregate load models represent the overall coordinated behaviour of individual electric and electronic components, such as motors, lighting, electrical appliances, etc. supplied by a common power system busbar [1]. The impact of the accurate representation of the steady-state and dynamic characteristics of power system loads has been long recognized and investigated both at the transmission and distribution network levels, especially considering studies pertaining to voltage and angular stability [2–6]. Nevertheless, in the last decades the increased penetration of motors and the introduction of new power electronic interfaced loads combined with the need for more operational flexibility as well as the application of advanced voltage and frequency control strategies in the distribution network have renewed the scientific interest on load modelling [7]. Although, detailed load models provide very accurate load representation, this method requires significant computational power and large simulation times for extended networks. However, detailed information of the real load characteristics is rarely available to transmission and distribution utilities. Thus, load busbars are represented by equivalent models representing the aggregation of different individual components, such as static, inductive and capacitive loads, motor driven consumers, etc. [1,6].

In aggregate load modelling there are two main approaches: the component-based and the measurement-based [8]. The former involves the derivation of an aggregate load model based on information from its constituent parts, including [8]: (a) the load class mix (industrial, agricultural, residential), (b) the composition of each of those classes (heating, cooling, air conditioning, etc.) and (c) characteristics of each load component related to the corresponding physical characteristics. The advantages of this approach are that it does not require field-measurements and that it can be easily applied to different bus substations [1]. However, the component-based approach is not considered accurate enough to represent the distinct load characteristics under various system disturbances. On the other hand, in the measurement-based approach the model parameters are typically defined a priori and their values are estimated using system identification techniques to fit the input–output data obtained from measurements. Significant

* Corresponding author. Tel.: +30 2541079568; fax: +30 2541079568.
E-mail address: thpapad@ee.duth.gr (T.A. Papadopoulos).

http://dx.doi.org/10.1016/j.epsr.2016.06.022
0378-7796/

advantages of the latter approach are: (a) load dynamics are directly captured in the derived models, thus presenting high fidelity and yielding more accurate and realistic system studies and (b) model parameters can be updated almost in real-time [9]. It should be noted at this point that this technique requires in situ measurements as well as the placement of measurement system at the load buses [1]. However, the advent of smart grids and the installation of phasor measurement units (PMUs) at transmission and distribution networks have enabled the measurement-based approach as more appealing than it was in the past [10,11].

Moreover, load models are mainly classified in static and dynamic models. Static load models are not dependent on time, thus they describe the relationship of the load real/reactive power at any time instant with the voltage and/or frequency [1,12,13]. On the other hand, dynamic load models express the load real/reactive power at any time instant as a function of the voltage and/or frequency of the present and past time instants. Static models are typically used to represent resistive, lighting, residential loads, etc., in steady-state calculations [1]. However, a recent study revealed that about 70% of the system utilities and operators worldwide also use static load models in dynamic power system studies [7].

Most of the existing static and dynamic modelling studies concentrate on the parameter estimation procedure of models, e.g. the polynomial [13], the exponential recovery (ER) [14,15], the composite [16] and the transfer function models [17]. However, most of these models consider only a simple form of load recovery after the disturbance, thus they cannot accurately represent more complex oscillatory cases of load dynamics. Another significant issue is that in most cases the derived load models are valid only for a given operating condition. Therefore, the model parameter estimation procedure must be repeated several times to account for different operating conditions.

Considering the above issues, the scope of the paper and its main contribution are to present a comprehensive identification procedure to derive generic measurement-based load models for simulating dynamic responses under a wide range of operating conditions.

Initially, in the proposed procedure the accuracy of the widely used polynomial and the ER load models of the first and second order are systematically investigated and proper criteria are proposed to determine their usability according to the load mix composition of the total load. To fulfil this objective, the training and validation data are generated using Monte Carlo simulations, assuming a combination of different types of dynamic loads and dynamic–static load mixture. Additionally, the application of the MultiStart routine is proposed to calculate the optimal solution for the estimation of the load model parameters [18].

Subsequently, for extending the applicability of the dynamic load models to different operating conditions and for developing generic load models, two methodologies are evaluated. The first methodology is based on the calculation of the mean characteristics [15], while the second is introduced for the first time in the archived literature and is based on artificial neural networks (ANN). Finally, the robustness of the developed generic models is evaluated under realistic operating conditions, following a systematic procedure that considers different noise levels.

2. Load models overview

2.1. Polynomial – ZIP model

One of the most wide spread static load model is the polynomial, which is also known as ZIP, since it consists of constant impedance (Z), current (I) and power (P) terms. Although the ZIP model is suitable for steady-state power system studies, still 19% of network operators and utilities worldwide are utilizing it in dynamic simulations [12]. It should be noted that the ZIP model is among the three most popular load models used for power systems analysis [7]. The formulation that relates the real (P) and reactive (Q) power to the bus voltage (V) is given in (1) and (2), respectively.

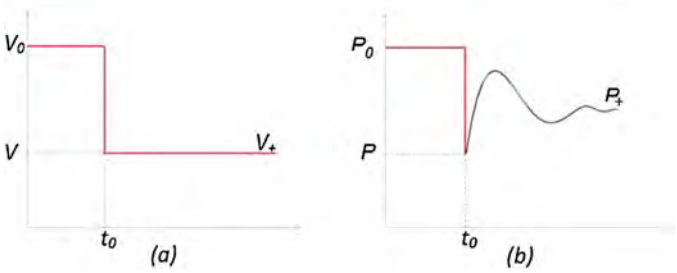

Fig. 1. General load response, (a) voltage disturbance, (b) real power response.

$$P_{ZIP} = P_0 \left[a_2 \left(\frac{V}{V_0} \right)^2 + a_1 \left(\frac{V}{V_0} \right) + a_0 \right] \quad (1)$$

$$Q_{ZIP} = Q_0 \left[b_2 \left(\frac{V}{V_0} \right)^2 + b_1 \left(\frac{V}{V_0} \right) + b_0 \right] \quad (2)$$

where V_0, P_0, and Q_0 are the steady-state pre-disturbance voltage, real and reactive power, respectively. With reference to (1) and (2) the parameters a_k and b_k correspond to the constant impedance load, current and power participation in the total load (for index k equal to 0, 1 and 2, respectively). Therefore, the sum of the corresponding parameters must be equal to unity.

2.2. Exponential recovery

In Fig. 1 the general form of the real power dynamic response $P_d(V)$ to a step change in the bus voltage V is presented. The response $P_d(V)$ can be analyzed into two terms as shown in (3) [14]. The first term pertains to the power response $P_t(V)$ that immediately follows the abrupt step of V. The second term embraces the gradual recovery element of the power response to a new steady-state value $P_s(V)$. The recovery $P_r(V)$ can be assumed of exponential form, while the size and the recovered steady-state are nonlinearly related to the bus voltage [1].

$$P_d(V) = P_t(V) + P_r(V). \quad (3)$$

Specifically, in their work Karlsson and Hill have used the general block diagram representation shown in Fig. 2 to express $P_d(V)$ [14]. The recovery term is described by the function N_{P_1} and the transfer function $G(s)$:

$$N_{P_1}(V) = P_s(V) - P_t(V) \quad (4)$$

$$G(s) = \frac{b_m s^m + b_{m-1} s^{m-1} + \cdots + b_0}{s^n + a_{n-1} s^{n-1} + \cdots + a_0} \quad (5)$$

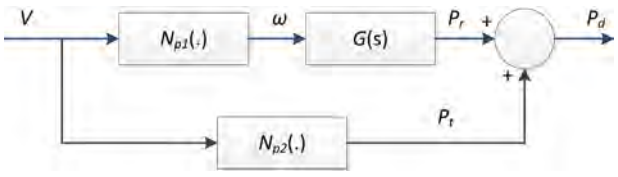

Fig. 2. Block diagram representation of the ER model.

Please cite this article in press as: K.S. Metallinos, et al., Derivation and evaluation of generic measurement-based dynamic load models, Electr. Power Syst. Res. (2016), http://dx.doi.org/10.1016/j.epsr.2016.06.022

where the nonlinear functions $P_t(V)$ and $P_s(V)$ that constitute the recovery term in (4) determine the steady-state and the transient power changes, described as follows:

$$P_t(V) = N_{P_2}(V) = P_0\left(\frac{V}{V_0}\right)^{\alpha_t} \quad (6)$$

$$P_s(V) = P_0\left(\frac{V}{V_0}\right)^{\alpha_s} \quad (7)$$

where α_t and α_s are the transient and steady-state real power exponents. Further details on this modelling procedure can be found in [14].

It is noted that $G(s)$ is strictly proper thus $m < n$. The transfer function $G(s)$ can be simplified according to the following assumptions:

- For $m = 0$ and $n = 1$, a 1st order representation is obtained, where $G(s)$ is written simply in the form of $G(s) = 1/(T_p s + 1)$, where T_p is the real power recovery time constant. This is the most popular formulation of the ER model used in power system studies [1,8,15,22]. *Note*: The formulation of this model in time-domain representation is described in Appendix.
- For $m = 1$ and $n = 2$, a 2nd order representation is obtained to describe more complex oscillatory power recovery responses.

The load recovery element P_r is given in state-space form, which for the case of the 2nd order form of the ER model is described as given in (8) [14].

$$\ddot{P}_r + a_1\dot{P}_r + a_0 P_r = b_1\dot{N}_{p_1}(V) + b_0 N_{p_1}(V). \quad (8)$$

Similar formulas are also obtained for the reactive power for the 1st and 2nd order ER models, following the same analysis. Specifically, the time-domain formulation of the 1st order ER model is presented in Appendix.

3. General modelling framework and test system description

It is reiterated that the scope of this paper is twofold: to evaluate the accuracy of the abovementioned load models and to develop generic load models, capable of simulating a wide range of operating conditions and load compositions. Therefore, the procedure followed involves two main stages, as analyzed in the flowchart of Fig. 3. As a first stage the parameters of the load models are identified using training data, while as a second stage generalized models suitable of representing a wide range of operating conditions are developed. The accuracy of the developed load models is evaluated, using the mean absolute percentage error (MAPE). Both the first and the second stage of the work are described in detail in Sections 4 and 5, respectively.

All data are generated using the test system depicted in Fig. 4. The examined power system is a real 132/11 kV substation of the Cypriot Power System modelled as an aggregated load at substation's secondary. The 11-kV bus is connected to the upstream grid through the 132/11.5 kV, 40 MVA, on-load tap changer transformer T1 that has 21% impedance and YNd11 connection. At the low-voltage (LV) side an artificial neutral point is provided by a 150 kVA earthing transformer. By using this configuration, several simulations are performed in DIgSILENT PowerFactory to investigate the influence of the voltage perturbations and load composition on load dynamics.

The aggregate load composition is constituted by two parts, i.e. the static and the dynamic. The dynamic part penetration to the total aggregate load is assumed variable, e.g. from 5% to 100% with a 5% step, whereas the static part changes accordingly to reach the 100% load mixture. In all cases the load power is constant and

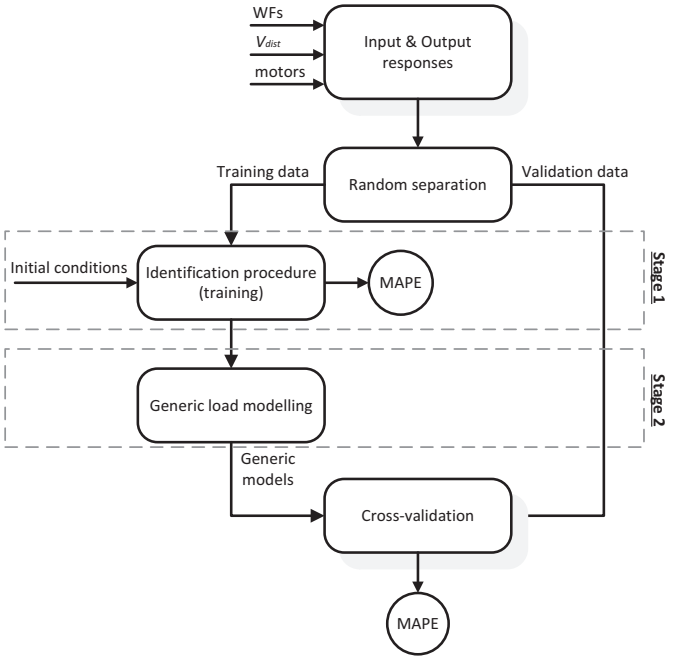

Fig. 3. Flowchart of identification procedure.

equals to 17.3 MVA. Therefore, there are $N_{ds} = 20$ possibilities for each dynamic–static combination. Moreover, to ensure that a wide range of load dynamics is considered, for each dynamic–static mixture the dynamic part is considered as the weighted average of $N_w = 7$ different LV motor loads as shown in (9a) and (9b).

$$P_{dynamic} = \sum_{i=1}^{7} w_i P_i \quad (9a)$$

$$Q_{dynamic} = \sum_{i=1}^{7} w_i Q_i \quad (9b)$$

where $P_{dynamic}$ and $Q_{dynamic}$ is the total dynamic load real and reactive power, respectively. The contribution of each motor type is determined by a weighting factor (WF) w_i, generated by Monte

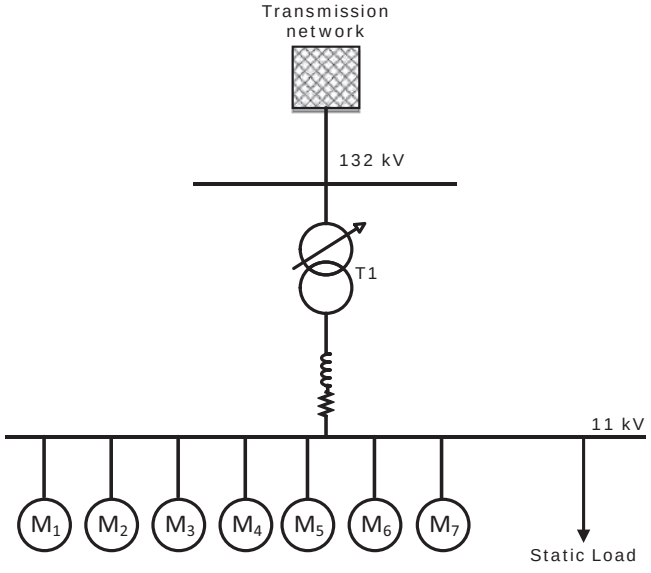

Fig. 4. One-line diagram of the substation modelled.

Please cite this article in press as: K.S. Metallinos, et al., Derivation and evaluation of generic measurement-based dynamic load models, Electr. Power Syst. Res. (2016), http://dx.doi.org/10.1016/j.epsr.2016.06.022

Carlo simulations assuming uniform distribution, whereas P_i and Q_i are the nominal real and reactive power of motor load i. WFs express the percentage of the different motor load types penetration in the total dynamic load part [19]. The examined LV motor loads include [12]: a small and a large industrial motor (M1 and M2), a water pump (M3), auxiliaries (M4), a weighted aggregate of residential motors (M5), a weighted aggregate of residential and industrial motors (M6) and a weighted aggregate of motors dominated by air conditioning (M7). Additionally, for each load composition different voltage perturbations at the substation secondary are caused in the range of 0.9625–1.0375 p.u., with respect to the nominal voltage, by changing the turns ratio of T1. The real and reactive power responses at the 11-kV bus, following the changes of the bus voltage are recorded. The number of the voltage samples is $N_v = 6$. Therefore, the total number of the generated samples is $N_t = N_{ds} \times N_w \times N_v = 840$ as the result of all possible combinations of motor load compositions, load types and voltage disturbances.

The available N_t dynamic responses are split into two groups corresponding to S and $N_t - S$ sets of responses. The first group of $S = 500$ sets is used as training data in the load identification process, while the remaining $N_t - S$ sets are used to cross-validate the robustness of the generic load models.

4. Parameter estimation and validation

4.1. Identification procedure

Typically, the load model parameters are estimated by means of non-linear least square (NLS) optimization. However, during the NLS process local optimal solutions may occur due to the inherent nonlinearity of the objective function, which depends significantly on the required initial guess of the model parameter values [16]. Therefore, the selection of the initial values of the load parameters is of crucial importance for the accurate performance of the developed model. Although, some initial estimation formulas have been proposed for the parameters of the 1st order form of the ER model [14], there is no reported similar procedure for the cases of the ZIP and the 2nd order form of the ER model. Therefore, the estimation of the load model parameters is performed by using the multistart algorithm that is available in MATLAB Global Optimization Toolbox to find the global optimum solution of the problem that leads to the best fit [18]. The methodology of the multistart algorithm employed is summarized in the following steps [18]:

Step 1) Generate multiple random starting points that follow uniform distribution.
Step 2) Run the local solver for all starting points. The local solver completes either when runs out of starting points or when the maximum number of iterations is reached.
Step 3) Solutions S_L are sorted from lowest to highest by the objective function value J_j, defined in (10).

$$J_j = \sum_{n=1}^{N} |(y[n] - \hat{y}[n])| \tag{10}$$

where $1 \le j \le S_L$, N is the total number of samples and $y[n]$ and $\hat{y}[n]$ are the measured and the estimated real/reactive responses of the nth sample, respectively. It is highlighted that as the number of the starting point increases, the possibility for multistart to converge to the global solution tends to unity. In this work, after several trials, the maximum number of iterations for the case of the ZIP and 1st order ER model is selected to 50 for all simulations, while for the 2nd order ER model the required number of iterations is 500. Among the available optimization solvers the trust-region NLS algorithm is selected [18].

Step 4) Loop over the L_s solutions beginning with the lowest (i.e. best) objective function value and find the S_F solutions satisfying both the following conditions:

$$|J_k - J_j| \le \varepsilon_y \times \max(1, J_j) \tag{11a}$$

$$|\theta_k - \theta_j| \le \varepsilon_n \times \max(1, n_j) \tag{11b}$$

where $1 \le k \le S_F$, ε_n and ε_y are the termination tolerance for θ and J, both having default values set to 10^{-6}.

Step 5) From the resulting S_F sets of parameters, the solution with the lowest (i.e. best) objective function value gives the final set of load model parameters.

Finally, all developed load models are evaluated on the training data set by calculating MAPE defined in (12).

$$MAPE = \frac{1}{N} \sum_{n=1}^{N} \left| \frac{(y[n] - \hat{y}[n])}{y[n]} \right|. \tag{12}$$

4.2. Results and validation

In Fig. 5a and b the summary of the MAPE values for the examined three load models is presented for the real and reactive power responses, respectively. For each dynamic–static composition from 5% to 100%, the average MAPE is calculated using the corresponding samples from the available training data set. Overall, the MAPE for all three examined models increases with the dynamic load penetration in the load mix. The two ER models give much better results than the static ZIP load model when simulating both the real and reactive power during the disturbances. In particular, the performance of the 1st order and the 2nd order form of the ER models are satisfactorily enough considering the simulation of the real power in all cases. For the simulation of the reactive power the 2nd order ER model gives slightly better results than the 1st order form, especially for cases with dynamic load participation higher than 70%. The results obtained with the ZIP model are not acceptable for the simulation of the reactive power response for cases characterized by dynamic load participation higher than 30%. For the real power the corresponding limit is considered at 50%.

Next, the influence of the voltage disturbance level on the simulation of the load responses is investigated. In Fig. 6a and b the MAPE of the real and reactive power is plotted against the penetration of the dynamic–static composition, respectively. Results are presented for simulations pertaining to the 1st order

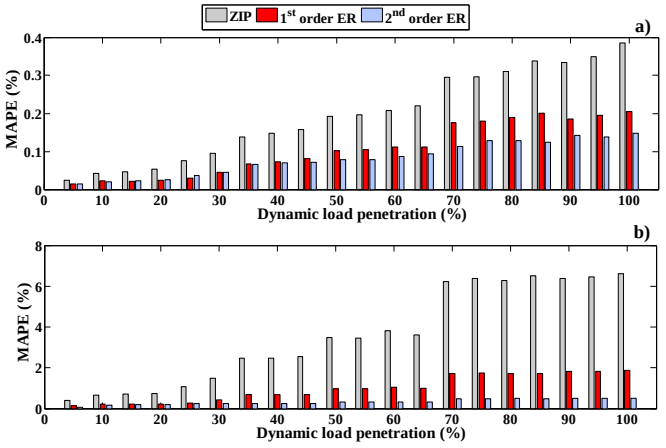

Fig. 5. MAPE for (a) real and (b) reactive power simulation using the three examined models.

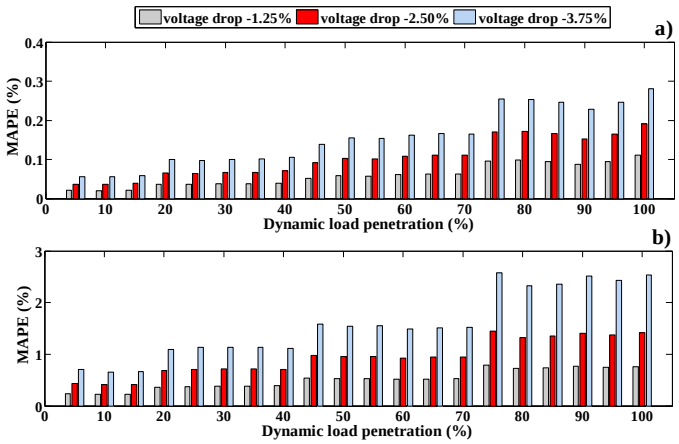

Fig. 6. MAPE of (a) real and (b) reactive power response for different disturbance levels – Simulations using the 1st order ER model.

form of the ER model. The dependence of the reactive power response on the voltage disturbance level is shown to be more significant than that of the real power. It is also shown that the error increases with the voltage disturbance level, especially for cases having dynamic–static composition higher than 30%. This behaviour reveals that the identified load model parameters can only be used for the simulation of dynamic studies, presenting small deviations in the disturbance levels [20].

Finally, the variation of the load model parameters due to the different loading conditions is examined [1]. The variation of the parameters for the 1st order form of the ER model against the dynamic load penetration for both real and reactive power is presented in Fig. 7. For each loading condition, the mean value of the corresponding model parameters identified from the available training data set is plotted. The results reveal that all model parameters are affected by the loading conditions, thus are only valid for the corresponding operating condition. As a consequence, the identified load parameters cannot be assumed generic and must be updated to represent the load characteristics for each case [1]. Similar conclusions for both of the above tests are also observed for simulations using the ZIP and the 2nd order form of the ER model.

5. Robust estimation of load parameters

5.1. Generic modelling approaches

In order to extend the applicability of the load models to account for more robust estimation of load parameters, i.e. to represent the typical load characteristics for cases different from those they have originally been developed using the available training data set, two generic modelling approaches are examined for the 1st and the 2nd order form of the ER model. The ZIP model is not included in the analysis, since its usability is rather limited, according to the results discussed in the previous section.

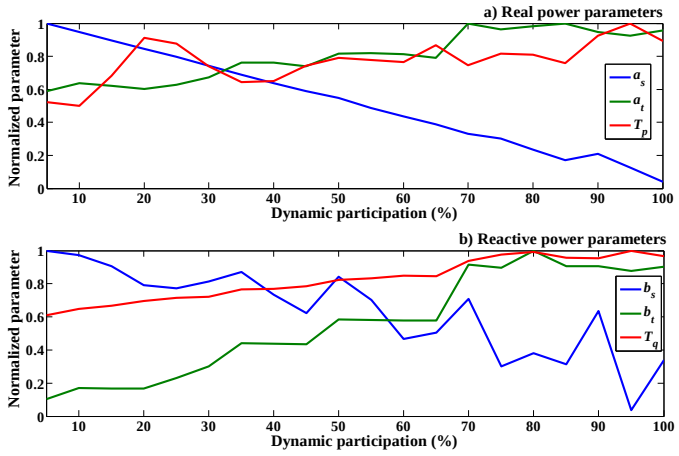

Fig. 7. Parameter variation against dynamic load participation.

In the first approach, the identified ER model parameters obtained from the training data are first categorized into four load mix composition groups $LMCG_\ell$, according to the dynamic load penetration. Index ℓ takes values 1, 2, 3 and 4. The range of the corresponding penetration levels for each group is 0–25%, 25–50%, 50–75% and 75–100%. Thus, $LMCG_1$ corresponds to the load mix group with the lowest dynamic load penetration, while $LMCG_4$ to the highest. Next, a representative/most probable set of parameters is obtained for each group by calculating the mean characteristics of the corresponding training data [15].

The second methodology is based on ANNs. An ANN is a group of interconnected nodes (neurons) which exchange messages to "learn" complex non-linear functions. The neuron is the building block of artificial neural networks and is a mathematical function designed as a representation model of biological neurons [23]. In general the ANN model consists of inputs, an output layer and a hidden layer in between. The hidden layer is a group of neurons acting as a transfer function to represent highly complex non-linear problems. The operation of ANNs per layer can be described by the following steps. Initially the influence of the input elements of the input vector **x** is weighted by weight vector **w**. Next, the bias vector **b** biases the weighted product using the sum operator, which gathers the weighted inputs and biases. Finally, the layer output signal is generated by passing the sum operator product to the transfer function f() as follows: $\mathbf{y} = f(\mathbf{w}^T\mathbf{x} + \mathbf{b})$. In case of hidden layers, the corresponding output is the input of the next layer and so on up to the output layer. Subsequently, through an iterative process, the elements of the weight vectors are modified appropriately to represent the influence of training data set, thus enabling the learning process.

Therefore, the developed ANN captures a general relation between the model inputs and outputs from a set of training patterns by successively adjusting the weights of the input–output interconnections in order to predict the load model parameters for new conditions. The inputs of the ANN are: (a) the percentage of the dynamic load in the total dynamic–static mixture, (b) the pre-disturbance load real (P_0) and (c) reactive (Q_0) power. The ANN outputs are the corresponding load model parameters.

Considering the design of an ANN, two critical parameters must be determined, i.e. the number of hidden layers and the number of neurons in each layer. Introducing several hidden layers leads to a high complexity network, without any substantial impact and also to longest training time requirements. Regarding the number of neurons per layer no specific rule for defining the optimum number of neurons in the hidden layer can be found in the literature, since this number depends on the number of inputs and the size of training data. Therefore, from the above remarks and after several tests a two-layer feed-forward ANN is proposed, consisting of a single hidden layer with 60 neurons and an output layer. The proposed ANN structure is shown in Fig. 8. The activation function of the output layer is the linear (purelin) to allow outputs to acquire any finite value, while in the hidden layer the tan-sigmoid (tansig) function is used.

The ANN training is carried out using the scaled conjugate gradient back propagation algorithm (trainscg) for a number of 500 iterations (epochs) with a target error of 10^{-5}. The trainscg algorithm is a variation of the classical backpropagation algorithm which is widely used in ANN training and performs well over a variety of problems, especially for networks with a large number of weights and has the competitive advantage over the other scaled

Please cite this article in press as: K.S. Metallinos, et al., Derivation and evaluation of generic measurement-based dynamic load models, Electr. Power Syst. Res. (2016), http://dx.doi.org/10.1016/j.epsr.2016.06.022

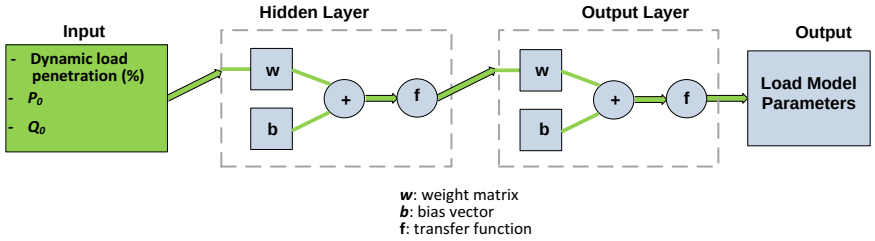

Fig. 8. ANN structure.

conjugate gradient algorithms that avoids the time-consuming line search [23].

5.2. Cross-validation

To evaluate the robustness of the developed generic models on a different set, the cross-validation technique is applied as illustrated in Fig. 3. The load model parameters obtained by following the two generic modelling approaches, are used to simulate the corresponding dynamic responses of the 1st and the 2nd order forms of the ER model, separately, from the validation data set. The cross-validation procedure is depicted in detail in Fig. 9.

Specifically, in Fig. 9a the resulting set of parameters derived from the training data are used to simulate representative load dynamic responses, characterizing each LMCG. The accuracy of the method is evaluated by comparing the representative load response of each LMCG to the corresponding validation set responses, characterized by similar dynamic load penetration levels to the former. Similarly, in Fig. 9b, since the ANN has been trained, P_0, Q_0 and the dynamic load percentage properties of the validation data load responses are used as inputs to generate ER load model parameters. The resulting parameters are used to regenerate the corresponding load response, which is compared to the original by means of MAPE.

The calculated validation error of the simulated responses for the 1st and the 2nd order form of the ER models is presented in Tables 1 and 2, respectively. Note, that the results for the ANN approach are grouped and presented into LMCG groups for consistency in the comparisons. From the results obtained using the 1st order form of the ER model, it is shown that although the ANN results in more accurate estimates in all cases, similar errors are calculated for both generic modelling approaches considering the real and reactive power, respectively. The MAPE is acceptable for the simulation of both the real and the reactive power responses, although in the first case is significantly lower. Considering the 2nd order form of the ER model similar conclusions can be obtained for the real power response. However, reactive power simulations present significant high levels of MAPE, showing that 2nd order ER model cannot be generalized. Comparing the results of the 1st and the 2nd order form of the ER model it is shown that both generic models exhibit high accuracy in the simulation of the real power load responses for both approaches as well as for all levels of dynamic load penetration.

6. Application to distorted responses

To evaluate the applicability of the proposed methodology to real-world conditions, some measured data are artificially created [21]. The real and reactive power responses generated by the ANN model for a 1.25% disturbance are distorted by additive white Gaussian noise (AWGN) and the proposed procedure to identify the 1st order ER model parameters is applied. The 1st order ER model is

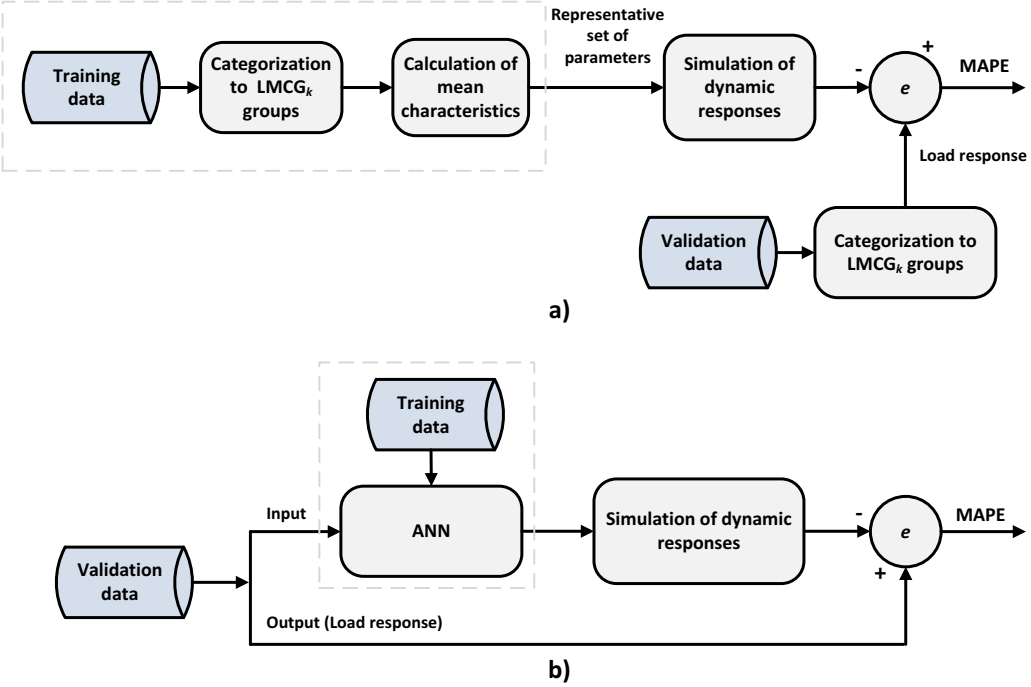

Fig. 9. Block diagram of cross-validation processes for the (a) mean characteristics and (b) ANN approaches.

Table 1
Validation MAPE for real and reactive power generic models using the 1st order form of the ER model.

Dynamic load participation	Mean characteristics approach		ANN approach	
	Real power	Reactive power	Real power	Reactive power
0–25%	0.28%	2.38%	0.122%	2.10%
25–50%	0.33%	1.55%	0.108%	1.54%
50–75%	0.25%	2.74%	0.191%	2.59%
75–100%	0.25%	4.09%	0.185%	4.20%

Table 2
Validation MAPE for real and reactive power generic models using the 2nd order form of the ER model.

Dynamic load participation	Mean characteristics approach		ANN approach	
	Real power	Reactive power	Real power	Reactive power
0–25%	0.26%	13.68%	0.08%	24.10%
25–50%	0.22%	53.75%	0.09%	45.32%
50–75%	0.23%	82.65%	0.15%	82.96%
75–100%	0.24%	115.41%	0.17%	119.27%

Table 3
Average values of the model parameters for the 1st order ER model.

Parameter	SNR						
	Noiseless	30 dB	25 dB	20 dB	15 dB	10 dB	5 dB
a_s	0.305	0.303	0.303	0.303	0.305	0.312	0.335
a_t	3.347	3.354	3.354	3.354	3.353	3.352	3.353
T_p	0.045	0.045	0.045	0.045	0.045	0.045	0.045
b_s	0.647	0.649	0.647	0.649	0.655	0.676	0.759
b_t	48.350	49.360	49.360	49.350	49.320	49.080	48.660
T_q	0.087	0.088	0.088	0.088	0.088	0.087	0.087

selected, since it can be generalized for both real and reactive power response. In this case the dynamic–static composition is considered 90%. The variance of AWGN is adjusted to represent different levels of signal-to-noise ratio (SNR) from 5 to 30 dB. For each noise level 100 Monte Carlo (MC) simulations are performed to statistically evaluate the accuracy of the mode estimates. Prior to parameter estimation, signal pre-processing is performed to improve the measured data quality [16]. The sampled real and reactive power responses are first low-pass filtered using finite impulse response (FIR) zero-phase low-pass filters (LPFs) of order 5 with cut-off frequencies at 20 Hz and subsequently are detrended to remove any drifts in the signal [22].

In Table 3 the resulting mean value of all estimated load model parameters are compared to the corresponding value of the noiseless case, whereas in Fig. 10 the relative standard deviation (RSD) of the load model estimates against SNR is plotted. For a_t, b_t, T_p and T_q the mean value of the parameter estimates can be practically assumed constant and the RSD increases slightly as the SNR decreases. Small deviations in the corresponding mean values are observed for a_s and b_s and especially for high noise levels, e.g. for SNR lower than 15 dB, where also significant RSD values are recorded. This is attributed to the fact that a_s and b_s are related to the steady-state condition prior to the disturbance, where variations in the steady-state signal due to noise cannot be easily eliminated through filtering. However, the results obtained are in general very close to the original values for all cases, verifying the robustness of the 1st order form of the ER model and of the proposed methodology considering the noise conditions.

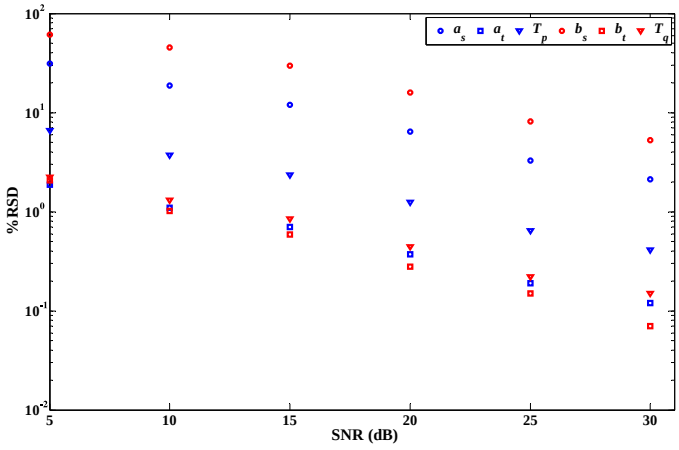

Fig. 10. Relative standard deviation of the load model estimates against SNR.

7. Conclusions

In this paper a comprehensive identification procedure to evaluate and develop generic load models is proposed. Towards this objective, the Monte Carlo method is adopted to generate training and validation data responses that represent a wide range of loading conditions and load mix compositions. Additionally, the Monte Carlo approach is used to generate random distorted data, in order to evaluate the performance of the developed models under realistic operating conditions. Thus, generic models that are efficient enough to simulate a wide range of operating conditions are proposed. In the first and simpler approach the load model parameters are calculated as the most possible/representative values for a specific range of dynamic load penetration. This approach could be similarly applied to develop representative sets of parameters based on seasonal categorization. The second approach is based on ANN, in which only the substation's real, reactive measurements and the dynamic load penetration are required.

Based on the comparative results it can be concluded that the ZIP model can be used in the simulation of dynamic real power studies in cases where the motor penetration is less than the static load participation mix. For reactive power simulation the motor penetration should not be more than one third of the total load mix. Both the 1st and the 2nd order form of the ER model can simulate satisfactorily the real and reactive power responses for any level of dynamic load penetration. However, for high levels of dynamic load penetration the 2nd order form of the ER model results in noteworthy improved estimates.

Considering the generic modelling approaches, validation results indicate that the developed generic models can generally provide satisfactory results in the simulation of both real and reactive power responses, when using the 1st order form formulation of the ER model. The additional transfer function parameters of 2nd

Please cite this article in press as: K.S. Metallinos, et al., Derivation and evaluation of generic measurement-based dynamic load models, Electr. Power Syst. Res. (2016), http://dx.doi.org/10.1016/j.epsr.2016.06.022

order form of the ER model do not result in significantly improved simulations of real-power responses compared to the 1st order form of the ER model. Considering the reactive power, the transfer function model parameters of high-order models are more sensitive to the system operating conditions and thus cannot be easily generalized. Therefore, generic 2nd order ER models should be used only for the accurate simulation of the oscillatory form of complex real power dynamic responses. Both the mean characteristics and ANN generic modelling approaches resulted into very accurate results for the real as well as the reactive power responses. Although the ANN modelling procedure is more complex, it takes into account in detail the influence of the network conditions via the input data and thus its application provides slightly more accurate results.

Appendix.

The real and reactive load power responses in time-domain for the 1st order ER model are expressed by (A.1) and (A.2), respectively [14,15].

$$P_d(t) = \left(P_0\left(\frac{V}{V_0}\right)^{a_s} - P_0\left(\frac{V}{V_0}\right)^{a_t}\right)(1 - e^{-t/T_p}) + P_0\left(\frac{V}{V_0}\right)^{a_t}, \quad \text{(A.1)}$$

$$Q_d(t) = \left(Q_0\left(\frac{V}{V_0}\right)^{b_s} - Q_0\left(\frac{V}{V_0}\right)^{b_t}\right)(1 - e^{-t/T_q}) + Q_0\left(\frac{V}{V_0}\right)^{b_t}, \quad \text{(A.2)}$$

The parameters of the real power response are defined in Section 2.2. For the reactive power response Q_0 is the reactive power consumption prior to the disturbance, T_q denotes the reactive power recovery time constant and b_s and b_t are the steady-state and transient reactive power voltage exponents, respectively.

References

[1] B.-K. Choi, H.-D. Chiang, Y. Li, Y.-T. Chen, D.-H. Huang, Measurement-based dynamic load models: derivation, comparisons, validation, IEEE Trans. Power Syst. 21 (3) (2006) 1276–1283.
[2] W. Mauricio, A. Semlyen, Effect of load characteristic on the dynamic stability of power systems, IEEE Trans. Power Appar. Syst. 91 (6) (1972) 295–2304.
[3] J.V. Milanovic, Overview, current trends and latest results in estimating the effects of load modelling on power-system damping and stability, Eur. Trans. Electr. Power 7 (2) (1997) 107–113.
[4] J.V. Milanovic, I.A. Hiskens, Effects of load dynamics on power system damping, IEEE Trans. Power Syst. 10 (2) (1995) 1022–1028.
[5] I.A. Hiskens, J.V. Milanovic, Load modelling in studies of power system damping, IEEE Trans. Power Syst. 10 (4) (1995) 1781–1788.
[6] E. Welfonder, H. Weber, B. Hall, Investigations of the frequency and voltage dependence of load part systems using a digital self-acting measuring and identification system, IEEE Trans. Power Syst. 4 (1) (1989) 19–25.
[7] J.V. Milanovic, K. Yamashita, S. Villanueva Martinez, S.Z. Djokic, L.M. Korunovic, International industry practice on power system load modeling, IEEE Trans. Power Syst. 28 (3) (2013) 3038–3046.
[8] I.R. Navaro, Dynamic load models for power systems (PhD thesis), Lund University, Sweden, 2002.
[9] P. Regulski, D.S. Vilchis-Rodriguez, S. Djurović, V. Terzija, Estimation of composite load model parameters using an improved particle swarm optimization method, IEEE Trans. Power Deliv. 30 (2) (2015) 553–560.
[10] V. Vignesh, S. Chakrabarti, S.C. Srivastava, Power system load modelling under large and small disturbances using phasor measurement units data, IET Gen. Transm. Distrib. 9 (12) (2015) 1316–1323.
[11] J.M. Ramirez, V. Benitez, Dynamic equivalents by RHONN, Electr. Power Compon. Syst. 35 (2007) 377–391.
[12] Bibliography on load models for power flow and dynamic performance simulation, IEEE Trans. Power Syst. 10 (February (1)) (1995) 523–538.
[13] Standard load models for power flow and dynamic performance simulation, IEEE Trans. Power Syst. 10 (3) (1995) 1302–1313.
[14] D. Karlsson, D.J. Hill, Modelling and identification of nonlinear dynamic loads in power systems, IEEE Trans. Power Syst. 9 (1) (1994) 157–166.
[15] D.P. Stojanovic, L.M. Korunovic, J.V. Milanovic, Dynamic load modeling based on measurements in medium voltage distribution network, Electr. Power Syst. Res. 78 (2008) 228–238.
[16] H.-D. Chiang, J.-C. Wang, C.-T. Huang, Y.-T. Chen, C.-H. Huang, Development of a dynamic ZIP-motor load model from on-line field measurements, Int. J. Electric. Power Energy Syst. 19 (7) (1997) 459–468.
[17] I.F. Visconti, D.A. Lima, J.M.C. de Sousa Costa, N.R.deB.C. Sobrinho, Measurement-based load modeling using transfer functions for dynamic simulations, IEEE Trans. Power Syst. 29 (1) (2014) 111–120.
[18] Global Optimization Toolbox: User's Guide. The Mathworks Inc., Natick, MA. [Online]. Available: www.mathworks.com/help/pdf_doc/ident/ident.pdf.
[19] Y. Xu, J.V. Milanović, Artificial-intelligence-based methodology for load disaggregation at bulk supply point, IEEE Trans. Power Syst. 30 (2) (2015) 795–803.
[20] V. Vignesh, S. Chakrabarti, S.C. Srivastava, Power system load modelling under large and small disturbances using phasor measurement units data, IET Gen. Transm. Distrib. 9 (12) (2015) 1316–1323.
[21] V. Knyazkin, C.A. Canizares, L.H. Soder, On the parameter estimation and modeling of aggregate power system loads, IEEE Trans. Power Syst. 19 (2) (2004) 1023–1031.
[22] T.A. Papadopoulos, E.N. Tzanidakis, P.N. Papadopoulos, P. Crolla, G.K. Papagiannis, G.M. Burt, Aggregate load modeling in microgrids using online measurements, in: MedPower, 3–7 November 2015, 2014.
[23] H. Demuth, M. Beale, M. Hagan, Neural Network Toolbox™ 6 User's Guide, The MathWorks, 2009.

Please cite this article in press as: K.S. Metallinos, et al., Derivation and evaluation of generic measurement-based dynamic load models, Electr. Power Syst. Res. (2016), http://dx.doi.org/10.1016/j.epsr.2016.06.022